Processes of equatorial thermal structure: An analysis of Galileo temperature profile with 3-D model

T. Majeed[1], J. H. Waite, Jr.[1], S. W. Bougher[1] and G. R. Gladstone[2]

Short title: EQUATORIAL THERMAL STRUCTURE

Abstract. The Jupiter Thermosphere General Circulation Model (JTGCM) calculates the global dynamical structure of Jupiter's thermosphere self-consistently with its global thermal structure and composition. The main heat source that drives the thermospheric flow is high-latitude Joule heating. A secondary source of heating is the auroral process of particle precipitation. Global simulations of Jovian thermospheric dynamics indicate strong neutral outflows from the auroral ovals with velocities up to $\sim$2 km/s and subsequent convergence and downwelling at the Jovian equator. Such circulation is shown to be an important process for transporting significant amounts of auroral energy to equatorial latitudes and for regulating the global heat budget in a manner consistent with the high thermospheric temperatures observed by the Galileo probe. Adiabatic compression of the neutral atmosphere resulting from downward motion is an important source of equatorial heating (< 0.06 μbar). The adiabatic heating continues to dominate between 0.06 and 0.2 μbar, but with an addition of comparable heating due to horizontal advection induced by the meridional flow. Thermal conduction plays an important role in transporting heat down to lower altitudes ($>0.2\mu$bar) where it is balanced by the cooling associated with the wind transport processes. Interestingly, we find that radiative cooling caused by H_3^+, CH_4, and C_2H_2 emissions does not play a significant role in interpreting the Galileo temperature profile.

1. Introduction

On December 8, 1995, the Atmospheric Structure Instrument (ASI) on the Galileo probe provided the first in-situ measurement of Jupiter's neutral atmospheric structure from 1029 km to 133 km (altitudes are referenced to 1-bar pressure level) near the Jovian equator (Lat: 6.5°; λ_{III}: 4.5°) [*Seiff et al.*, 1998]. The derived temperature profile exhibited wave-like variations and increased from $\sim$ 200 K at 400 km to about 950 K at 1000 km, consistent with the profile inferred from the solar and stellar occultation experiments performed during the Voyager flybys in 1979 [*Festou et al.*, 1981; *Atreya et al.*, 1981]. H_3^+ emissions from the Jovian auroral and equatorial regions also provide information on the neutral temperature structure [*Drossart et al.*, 1989]. Analysis of such observations from the Canada-France-Hawii Telescope (CFHT) by *Marten et al.* [1994] yielded an exospheric temperature of 800$\pm$100 K near the Jovian equator. *Hubbard et al.* [1995] observed the occultation of the star SAO 78505 by Jupiter at $\sim$ 8° latitude and determined a temperature of 176$\pm$12 K, in good agreement with the ASI temperature at a pressure level of 1.8 μbar. *Liu and Dalgarno* [1996] found an atmospheric temperature of 500$\pm$30 K at 0.3 μbar for a best fit to the Hopkins Ultraviolet Telescope (HUT) dayglow observation. Table 1 shows a summary of equatorial temperatures for Jupiter's upper atmosphere inferred from the above data.

The observed temperature structure indicates that exospheric temperatures at Jupiter cannot be maintained by solar EUV heating alone [*Strobel and Smith*, 1973]. Dissipation of gravity waves [*Matcheva and Strobel*, 1999; *Young et al.*, 1997; *Yelle et*

al., 1996], soft and energetic particle precipitation [*Hunten and Dessler,* 1977; *Waite et al.*, 1997], and transport of auroral heat to low latitudes by thermospheric winds [e.g., *Waite et al.*, 1983] have all been proposed as mechanisms for heating the upper atmosphere.

2. Existing Interpretation of Galileo Temperature Profile

Young et al. [1997] determined that the dissipation of upward-propagating internal gravity waves could produce enough heat to account for the high thermospheric temperatures measured by the Galileo probe. While *Matcheva and Strobel* [1999] and *Hickey et al.* [2000] argued that the propagation of gravity waves identified in the probe data can certainly heat the upper thermosphere, they proposed that the downward flux of sensible heat from the dissipating waves causes an appreciable cooling. Thus, the net heating rate from the observed propagating gravity waves was insufficient to maintain the high Jovian thermospheric temperatures.

Independently, *Waite et al.* [1997] modeled the energetics of Jupiter's upper atmosphere based on charged particles precipitating from the inner radiation belt to the Jovian equatorial atmosphere, resulting in X-ray emissions consistent with those observed by the High Resolution Imager on the Rontgensatellit (ROSAT). The model calculations of altitude profiles of the heating rates suggested that the energy associated with the observed low-latitude X-ray brightness could be an important source of upper atmospheric heating and could account for Jupiter's high thermospheric temperatures. However, *Maurellis et al.* [2000] argued that a major fraction of the low-latitude

Jovian X-ray emissions is due to solar scattering and fluorescence, and therefore cannot provide enough energy for the upper atmospheric heating. Recent X-ray observations of Jupiter with Chandra [*Gladstone et al.*, 2002] appear to support the scattered sunlight hypothesis, although there are some non-uniformities in the emission that could be indicative of charged-particle precipitation.

The model calculations performed by *Sommeria et al.* [1995] have indicated that an extremely rapid auroral electrojet can generate supersonic neutral winds up to 20 km/s and could disperse high-latitude auroral heating globally through a strong meridional flow to explain high Jovian exospheric temperatures. However, there is no observational evidence to date for winds of such magnitude. The first 3-D Jovian Ionospheric Model (JIM), developed by *Achilleos et al.* [1998], demonstrated that some of the energy deposited by high-latitude processes in the auroral regions can be transported to the Jovian equator by the meridional circulation of the neutral flow, yielding an equatorial temperature profile near local noon with an exospheric temperature of 1200 K [*Millward et al.*, 2002].

Independently, we have developed a 3-D Jupiter Thermospheric General Circulation Model (JTGCM) to simulate the Jovian thermospheric winds self-consistently with global temperature and ion-neutral species distributions. An important goal of our model is to study the response of imposed high-latitude ion convection, along with particle and Joule heating, on the neutral flow, and its subsequent impact on the thermal structure. The details of the JTGCM, including the model inputs and global simulations of thermospheric dynamics and temperatures, are reported elsewhere [*Bougher et al.*,

2004]. In this paper, we present the JTGCM analysis of the vertical thermal structure in comparison with that observed by the Galileo probe near the Jovian equator. We discuss heating and cooling processes within the equatorial region which indicate that the transport of significant amounts of auroral energy by high-speed neutral winds is responsible for maintaining the measured temperatures at the probe location.

3. The JTGCM

The JTGCM uses a 5° latitude by 5° longitude grid with 39 vertical pressure layers in increments of 0.5 pressure scale heights. The model solves coupled thermodynamic, zonal momentum, meridional momentum, continuity, and hydrostatic equations self-consistently using the basic framework of the National Center for Atmospheric Research (NCAR) general circulation model. Each of these equations is cast in log-pressure coordinates ($Z_p = \ln(p_0/p)$), with a specified reference pressure level corresponding approximately to the average homopause level. For the JTGCM code, this reference pressure is located at 4.5 μbar ($Z_p = 0$). Each Z_p interval corresponds to a 1-scale height (at the local temperature).

The lower boundary in the JTGCM is at 20 μbar, to take into account the hydrocarbon cooling due to C_2H_2 and CH_4 near the homopause level. Lower boundary conditions for temperature and neutral densities are taken from Galileo [*Seiff et al.*, 1998] and Voyager data [*Festou et al.*, 1981]. Upper boundary conditions were specified at $\sim 1.1\times 10^{-4}$ nbar in order to properly include high-altitude auroral heating processes [*Ajello et al.*, 2001; *Grodent et al.*, 2001] and H_3^+ cooling in the near-IR [*Drossart*

et al., 1993]. Boundary conditions for temperature, neutral densities, and winds are taken from the corresponding NCAR terrestrial Thermosphere Ionosphere General Circulation Model (TIGCM) [*Roble et al.*, 1988]. A convection electric field is estimated and corresponding ion drifts (u_i and v_i) are generated using an ionospheric convection model based on Voyager measurements of ion convection in the outer magnetosphere [cf. *Eviatar and Barbosa*, 1984] mapped to high latitudes using the VIP4 magnetic field model [*Connerney et al.*, 1998].

The JTGCM uses solar EUV radiation as a source of equatorial heating, while the particle heating calculated by *Grodent et al.* [2001] (incident electron energy spectrum described by a combination of three Maxwellian distribution functions with total particle energy $E_o = 25$ keV and energy flux ~ 110 ergs cm^{-2} s^{-1}) is used for the auroral region. The solar source is specified within a narrow band of $\pm 10°$ latitude. The auroral heating by particle precipitation is specified along the polar ovals, which are currently described by the auroral morphology deduced from analysis of WFPC2 images taken in 1996 and 1997 [*Clarke et al.*, 1998]. Recent analysis of HST-STIS images by *Grodent et al.* [2003] indicates that the auroral oval locations on Jupiter are constant in latitude and system III longitude.

Ion-drag within the JTGCM code is described as a dominant physical process which limits neutral wind speeds through couplings between ions in the Jovian auroral ovals and the co-rotating neutral atmosphere. The ions, magnetically connected to the sub-rotating regions of the magnetosphere, lose their momentum in collisions with neutrals and thus drive the neutrals to move in roughly the same direction. This drag

peaks near the height of maximum ion density. At higher ionospheric heights the effect of ion-drag gradually decreases as the ion gyrofrequency exceeds the ion-neutral collision frequency which constraints ionization to move along magnetic field lines. Joule heating, which is driven by the differential velocity between the ion and neutral species in the auroral ionosphere, has also been described in the JTGCM code as an important mechanism for modifying Jupiter's global thermospheric winds and temperatures. The parameterization of ion-drag and Joule heating in the JTGCM code is based on the formulation described by *Roble and Ridley* [1987]. The long-term effects of energy transport on the equatorial thermal structure are assessed by simulating the Jovian dynamics for more than 60 planetary rotations, until a cyclic steady-state solution in the modeled fields (i.e., the global 3-component neutral winds and corresponding temperatures and density distributions) is achieved.

4. Results and Discussion

The global temperature simulation with auroral forcing of particle precipitation alone does not provide sufficient energy to account for the temperature structure observed by the Galileo probe. The steady-state temperature fields for an integration time of 60 Jupiter days indicate gradual cooling of the high-latitude auroral thermosphere in response to local pressure gradients which drive neutral winds away from the heated regions. The derived horizontal winds up to 1 km/s served to reduce auroral temperature in the exospheric region from 1000 K at the start of the simulation to around 600-700 K at the end of the simulation. An equatorial temperature as high as 450 K, although

a factor of 2 cooler than the measured one, clearly indicates that the energy has been transported out of the auroral regions by a strong meridional flow. But we need an additional source of energy to explain the measured characteristics of the thermal profile.

Figure 1 shows the simulation of zonally-averaged temperatures with the best case scenario, which includes an auroral forcing by particle heating and an additional forcing by 15% of the total Joule heating produced in the auroral ovals. The simulation was run for 62 Jupiter rotations to achieve steady-state temperature fields. Note that the neutral temperature is quite uniformly distributed globally for the thermospheric heights with pressure $>$ 4 nbar (or zp$<$7) with the exception of the high-latitude region near the southern pole (70-90°S). This ambiguous behavior of temperature seems to reflect strong ion-drag forcing due to the magnitude of zonally-averaged ion winds (u_i) in the southern auroral oval, which is about a factor of 2 larger than in the northern auroral oval. Thus, ion-drag together with Joule heating effectively enhances momentum transfer affecting the neutral winds and temperatures.

In the upper thermospheric regions (pressure $<$ 4nbar or zp $>$ 7), horizontal winds up to 1.8 km/s, driven largely by additional Joule heating, appear to be responsible for creating strong upwelling and divergence of the neutral flow in the polar regions, while convergence and subsidence of this flow is seen at the Jovian equator. Such a global circulation of neutral flow results in an increase in neutral temperatures throughout the thermosphere compared to the case with particle heating alone. Joule heating dominates heat budgets in both hemispheres, yielding exospheric temperatures of 1000 – 1100 K

in the auroral regions, while the temperature near the Jovian equator is ~850 K (see Figure 1).

In Figure 2 we compare the JTGCM temperature profiles, simulated at the entry location of the Galileo probe, with the measured and modeled thermal structure from various sources listed in Table 1. Curve B shows a steady-state equatorial temperature profile with intense auroral heating caused by precipitated charged particles and solar EUV heating around the Jovian equator. In this simulation, the transport processes associated with the Jovian wind system provided sufficient cooling to the entire thermosphere to generate an exospheric temperature of ~490 K, which is about 60% cooler than the actual temperature measured by the Galileo ASI instrument (Curve A). Clearly, an additional source of energy is needed to explain the measured temperature profile.

Curve C shows a reasonable fit to the Galileo temperature profile by assuming 15% of the total Joule heating produced in auroral ovals. The JTGCM simulated temperatures at 0.1 and 0.01 nbar are also found to be in reasonably good agreement with those inferred from the analysis of CFHT high-resolution H_3^+ emission spectra [*Marten et al.*, 1994] and Voyager UVS solar occultation data [*Atreya et al.*, 1981], respectively. Furthermore, the model temperatures in the stratospheric region (between 1 and 2 μbar) also appear to be fairly close to the measured temperatures. However, an isothermal layer of $\sim$ 115 K between 1 and 10 μbar, simulated by the JTGCM, is considerably cooler than the temperature measured by Galileo, which suggests that the heat conducted downward in the model is radiated away too efficiently.

In the region between 1 and 0.01 μbar, the JTGCM predicts rapidly rising temperatures as the meridional flow of auroral winds carries auroral energy to lower latitudes. A similar rapid rise can be seen in the measured temperature, which has large vertical temperature gradients with a peak value of $\sim$3 K/km at 0.3 μbar [cf., *Sieff et al.,* 1998]. However, our model predicts a peak value of about 5 K/km at 0.3 μbar in the altitude profile of the temperature gradient. At the ASI probe location, our model predicts an integrated energy flux of $\sim$ 6 ergs cm^{-2} s^{-1} from meridional transport and heat conduction. This value is almost a factor of five larger than that used analytically by *Yelle et al.* [1996] to explain the measured temperatures at 10 nbar [*Marten et al.,* 1994] and 0.4 μbar [*Liu and Dalgarno,* 1996] by assuming energy from dissipating gravity waves alone. Clearly, dynamical sources of heat transport play an important role in our understanding of the bulk of the equatorial heat budget. The effects of excess Joule heating on the heat transport processes, which control the thermospheric temperatures have also been studied. Curve D shows an example of the equatorial temperature profile from the simulation which assumes twice the Joule heating compared to the one which explains the Galileo temperature profile. In this case, the exospheric temperature reaches up to 1880 K as a result of increased meridional transport of auroral heat to the entry location of the Galileo probe.

Figure 2 also shows a comparison between the equatorial temperature profiles derived from the JIM (Curve E) and JTGCM simulations. While the energy transport from the auroral ovals down to the equatorial region by neutral winds has been demonstrated by both models, the deficit in cooling rate due possibly to transport

processes and/or due to the absence of hydrocarbon and H_3^+ radiative cooling in JIM allows atmospheric heating to rapidly elevate the neutral temperature from 400 K at the lower boundary (2 μbar) to about 1200 K at exospheric heights.

In Figure 3 we show the vertical profiles of transport sources for thermospheric heating and cooling from the JTGCM simulation which best describes the thermal structure measured in-situ by the Galileo probe. Note that the contributing solar EUV energy source for the upper thermospheric heating is negligibly small, but is included in the model for completeness. Figure 3a illustrates the balance between adiabatic heating, caused by the downward flow of the neutral atmosphere, and cooling by thermal conduction. Certainly, this balance plays an important role in maintaining an exospheric temperature of ~890 K, consistent with observed temperature. In the region between 0.2 μbar and 1 nbar, the Jovian wind system seems to play an active role in transporting energy from the auroral region to the equatorial region. Figure 3b shows that the adiabatic process continues to dominate the heat budget, with a peak value of $\sim 5\times10^4$ eV cm^{-3} s^{-1} at 0.06 μbar. While horizontal advection, induced by meridional flow with a maximum velocity of ~55 m/s [*Bougher et al.*, 2004], becomes an important source of heating at 0.1 μbar, the process of heat conduction tends to cool down the atmosphere up to a pressure level of 0.2 μbar, with a maximum cooling rate of $\sim 3\times10^4$ eV cm^{-3} s^{-1}. Thus, the net heating rate is overwhelmed by transport sources, yielding a rapid increase in equatorial temperatures between 0.2 μbar and 0.01 μbar level (see Figure 2).

Figure 3c reveals the importance of vertical energy transport by thermal conduction

in the Jovian thermosphere from 1 to 0.2 μbar. The maximum heating rate for this region is about 3×10^5 eV cm^{-3} s^{-1}, which is primarily balanced by the cooling associated with wind transport processes. However, in the high-pressure regions (>1 μbar) of Jupiter's thermosphere, adiabatic cooling from atmospheric expansion is overwhelmed by other cooling sources. The effect of such a large net cooling rate on the background atmosphere has been demonstrated by the simulated temperature profile (Curve C in Figure 2), indicating cooler temperatures compared to those inferred from most of the observations in that region.

We estimate that the time constant for energy transport at 0.06 μbar is about 2×10^6 s from $\tau_T = c_p\rho T/q_T$, where q_T is the total heating rate in ergs cm^{-3} s^{-1} from all sources, as shown in Figure 3. c_p (1.4×10^8 ergs K^{-1} g^{-1}) and ρ (2.36×10^{-12} g cm^{-3}) are specific heat and atmospheric density, respectively, appropriate for an H_2 atmosphere with a temperature of 634 K. The corresponding time constant for cooling is estimated to be about a factor of two longer than the heating time constant. This suggests that the energy transport by meridional flow, with a speed roughly estimated as $R_j/\tau_T \sim 35$ m/s (R_j being Jupiter's radius) [*Bougher et al.*, 2004], should not be lost to downward conduction along the way to the Jovian equator.

5. Summary

The global dynamical structure of the Jovian thermosphere is simulated self-consistently with thermal structure and composition distributions using a three-dimensional Jupiter Thermosphere General Circulation Model (JTGCM). We have

shown that the global circulation of the neutral wind system, driven by auroral heating and 15% of the total Joule heating produced in the auroral ovals, can transport sufficient energy near the Jovian equator to explain the thermal structure observed by the Galileo probe. The energy transport processes associated with the Jovian wind system play a significant role in the global distribution of neutral temperatures. The cooling of auroral regions is caused by strong outflows which develop near the ovals as a result of large-scale pressure gradients and magnetospheric forcing imposed by the high-latitude ion convection. It is shown that the pole-to-equator circulation of the neutral flow resulting from strong Coriolis torques acting on the equatorward-directed meridional wind, rising motion in the auroral ovals, and subsequent convergence and downwelling motion at the Jovian equator, can regulate the transport of energy outward from the auroral regions to the rest of the planet. We find that such circulation controls the energy budget for the thermosphere at the location of the Galileo probe experiment. The heating is provided by the transport sources such as adiabatic and hydrodynamic advection for the upper thermosphere (<0.2 μbar), while the adiabatic cooling dominates the lower thermosphere. Cooling by H_3^+, CH_4, and C_2H_2 does not play a significant role in interpreting the measured temperature profile.

Acknowledgments. We would like to thank A. Ridley and D. Grodent for developing an ionospheric convection model. This work is supported by NASA grant NAG 5-11031 and NSF grant AST-0300005.

References

Achilleos, N. S., et al., JIM: A time-dependent, three-dimensional model of Jupiter's thermosphere and ionosphere, *J. Geophys. Res., 103*, 20,089, 1998.

Ajello et al., Spectroscopic evidence for high altitude aurora at Jupiter from Galileo extreme ultraviolet spectrometer and Hopkins ultraviolet telescope observations, *Icarus, 152*, 151, 2001

Atreya, S. K., T. M. Donahue, M. Festou, Jupiter – Thermal structure and composition of the upper atmosphere, *Astrophys. J., 247,* L43-L47, 1981.

with coupled dynamics and composition, *Icarus, 73*, 545, 1988.

Bougher, S. W., J. H. Waite, T. Majeed and G. R. Gladstone, Jupiter Thermosphere General Circulation Model (JTGCM): II. Global studies and dynamics driven by auroral and Joule heating, *J. Geophys. Res.,* To be submitted, 2003.

Clarke, J. T., et al., Hubble Space Telescope imaging of Jupiter's UV aurora during the Galileo orbiter mission, *J. Geophys. Res., 103,* 20,217, 1998.

Connerney J. E. P., M. H. Acuna, N. F. Ness, and T. Satoh, New models of Jupiter's magnetic fields constrained by the Io flux tube footprint, *J. Geophys. Res.,103,* 11,929, 1998.

Drossart, P., et al., Thermal profiles in the auroral regions of Jupiter, *J. Geophys. Res., 98,* 18,803, 1993.

Eviatar, A., and A. D. Barbosa, Jovian magnetospheric neutral wind and auroral precipitation flux, *J. Geophys. Res., 89,* 7393, 1984.

Festou, M., et al., Composition and thermal profile of the Jovian upper atmosphere determined by the Voyager stellar occultation experiments, *J. Geophys. Res., 86,* 5715, 1981.

Gladstone, G. R., et al., A pulsating auroral X-ray hot spot on Jupiter, *Nature,* 415, 1000.

Grodent, D., J. H. Waite, Jr., and J-C. Gerard, A self-consistent model of the Jovian auroral thermal structure, *J. Geophys. Res., 106*, 12,933, press, 2001.

Grodent, D., J. T. Clarke, J. Kim, J. H. Waite, and S. W. H. Cowley, Jupiter's main auroral oval observed with HST-STIS, *J. Geophys. Res.,108*, SMP 2-1, 2003.

Hickey, M. P., R. L. Walterscheid, G. Schubert, Gravity wave heating and cooling in Jupiter's thermosphere, *Icarus, 148,* 266, 2000.

Hubbard, W. B., V. Hammerle, C. C. Porco, G. H. Rieke, and M. J. Rieke, The occultation of SAO 78505 by Jupiter, *Icarus, 113,* 103, 1995.

Hunten, D. M., and A. J. Dessler, Soft electrons as a possible heat source for Jupiter's thermosphere, *Planet. Space Sci., 25,* 817, 1977.

Liu, W. and A. Dalgarno, The ultraviolet spectrum of the Jovian dayglow, *Astrophys. J., 462,* 502, 1996.

Marten, A., C. DeBergh, T. Owen, D. Gautier, J. P. Maillard, P. Drossart, B. L. Lutz, and G. S. Orton, Four micron high-resolution spectra of Jupiter in the North Equatorial Belt: H_3^+ emissions and ^{1}2C/^{1}3C ratio, *Planet. Space Sci., 42,* 391, 1994.

Matcheva, K. I., and D. F. Strobel, Heating of Jupiter's thermosphere by dissipation of gravity waves due to molecular viscosity and heat conduction, *Icarus, 140,* 328, 1999.

Maurellis, A. N., T. E. Cravens, G. R. Gladstone, J. H. Waite, and L. W. Acton, Jovian X-ray emission from solar X-ray scattering, *Geophys. Res. Lett., 27,* 1339, 2000.

Millward, G. H., et al., On the dynamics of the Jovian ionosphere and thermosphere III. The modelling of auroral conductivity, *Icarus, 160,* 95, 2002.

Roble, R. G., and E. C. Ridley, An auroral model for the NCAR thermospheric general circulation model (TGCM), *Ann. Geophysicae, 5A,* 369, 1987.

Roble, R. G. et al., A coupled thermospheric-ionospheric general circulation model, *Geophys. Res. Lett., 15,* 1325, 1988.

Seiff, A., et al., Thermal structure of Jupiter's atmosphere near the edge of a 5-μm hot spot in the north equatorial belt, *J. Geophys. Res., 103,* 22,857, 1998.

Sommeria, J., L. Ben-Jaffel, and R. Prange, On the existence of supersonic jets in the upper atmosphere of Jupiter, *Icarus, 119,* 2, 1995.

Strobel, D. F., and G. R. Smith, On the temperature of the Jovian thermosphere, *J. Atmos. Sci., 30,* 489, 1973

Waite, J. H., Jr., T. E. Cravens, J. U. Kozyra, A. F. Nagy, S. K. Atreya, and R. H. Chen, *J. Geophys. Res., 88,* 6143, 1983.

Waite, J. H. et al., Equatorial x-ray emissions: Implications of Jupiter's high exospheric temperatures. *Science, 276,* 104, 1997.

Yelle, R. V. et al., Structure of Jupiter's upper atmosphere: Prediction for Galileo, *J. Geophys. Res., 101,* 2149, 1996.

Young, L. A., R. V. Yelle, R. Young, A. Sieff, and D. B. Kirk, Gravity waves in Jupiter's thermosphere, *Science, 276,* 108, 1997.

T. Majeed, University of Michigan, Ann Arbor, MI. (tariqm@umich.edu)

J. H. Waite, Jr., University of Michigan, Ann Arbor, MI. (hunterw@umich.edu)

S. W. Bougher, University of Michigan, Ann Arbor, MI. (steveb@umich.edu)

G. R. Gladstone, Southwest Research Institute, San Antonio, TX (rgladstone@.swri.edu)

Received _____

[1]University of Michigan, Ann Arbor, MI 48109, U. S. A

[2]Southwest Research Institute, San Antonio, TX 78240, U. S. A

CAPTIONS

Figure 1. The JTGCM contours of zonally-averaged temperatures are shown as a function of latitude and pressure.

Figure 2. The JTGCM temperature profiles (Curve B, C, and D) are shown in comparison with the equatorial temperature profiles from JIM (Curve E) and *in-situ* measurements by the Galileo ASI probe (Curve A). Remotely-sensed temperature observations from various sources are also shown.

Figure 3. The JTGCM heating and cooling rates corresponding to Curve C of Figure 2 for the entry location of the Galileo ASI probe.

Table 1. Summary of observations.

Date	Experiment	Payload	Latitude (deg)	Temperature (K)	Pressure (bar)	Reference
3/5/79	Solar occultation	Voyager 1	12.0 N	1100 ± 200	$\sim 10^{-11}$	Atreya et al. (1979)
7/9/79	Stellar occultation	Voyager 2	14.5 N	200 ±30	$\sim 10^{-6}$	Festou et al. (1981)
7/9/79	Stellar occultation	Voyager 2	14.5 N	425 ±25	$\sim 3 \times 10^{-10}$	Festou et al. (1981)
3/92	Spectroscopy	CFHT	10.0 N	800 ±100	$\sim 10^{-11}$	Marten et al. (1994)
3/4/95	UV dayglow	HUT	1.0 N	530 ±70	$\sim 3 \times 10^{-7}$	Liu & Dalgarno (1995)
12/13/89	Stellar occultation	Groundbased	8.0 N	176 ±12	$\sim 2 \times 10^{-6}$	Hubbard et al. (1995)
12/8/95	ASI probe	Galileo	6.5 N	Profile	-36–9.5×10^{-10}	Seiff et al. (1998)

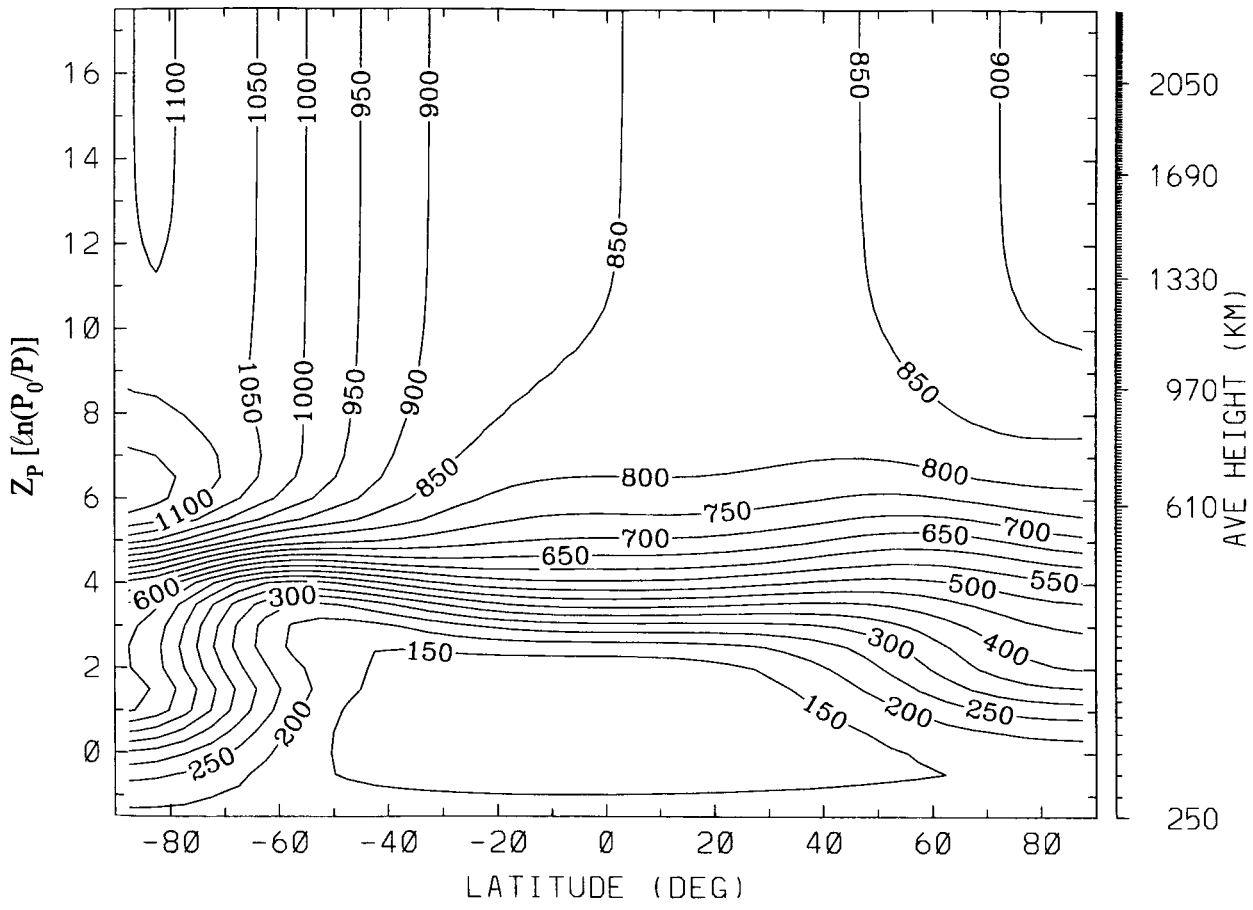
Z_P [ln(P_0/P)]
16
14
12
10
8
6
4
2
0
1100
1050
1000
950
900
850
800
750
700
650
600
550
500
400
300
250
200
150
-80
-60
-40
-20
0
20
40
60
80
LATITUDE (DEG)
2050
1690
1330
970
610
250
AVE HEIGHT (KM)

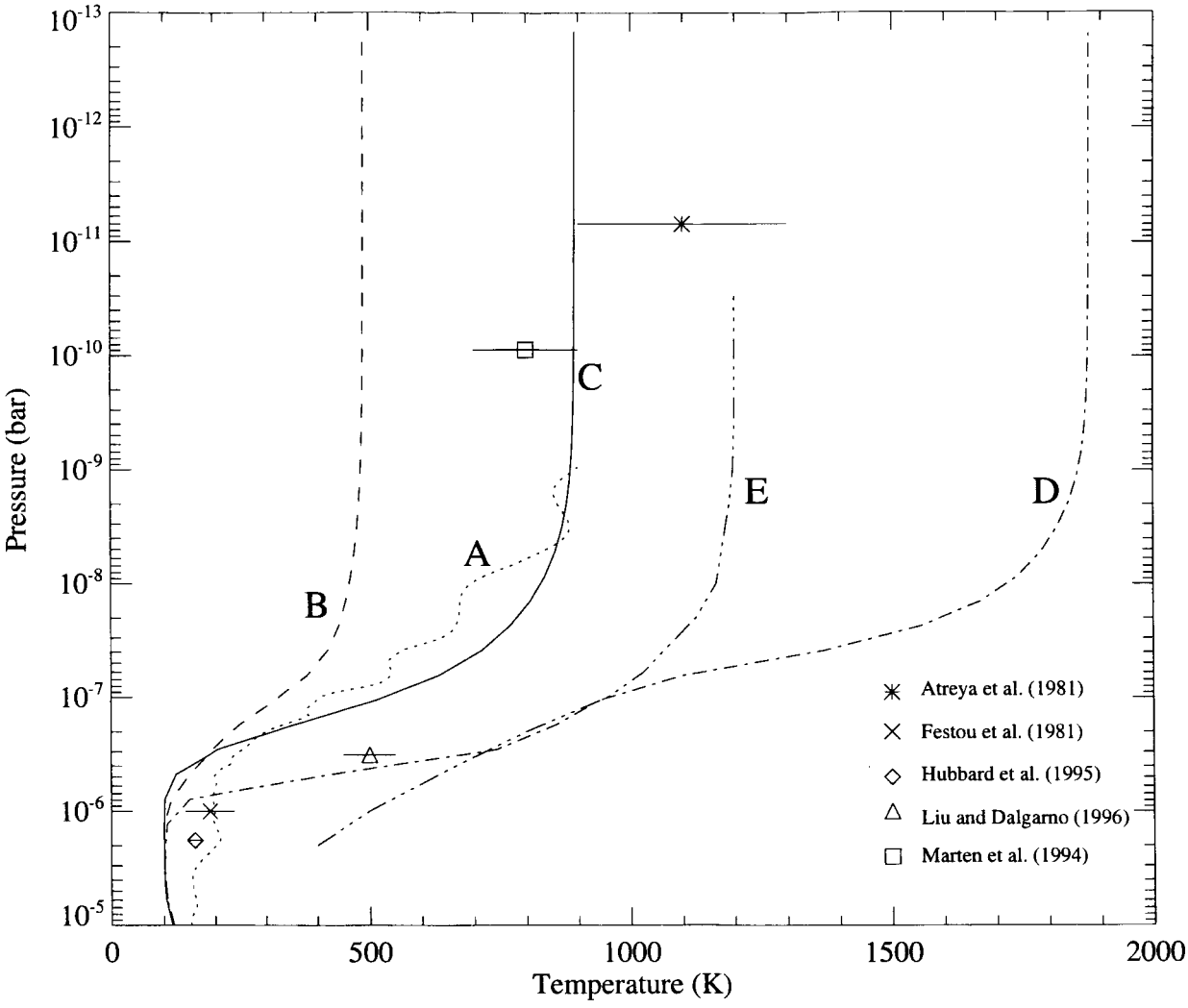
Pressure (bar)
10^{-13}
10^{-12}
10^{-11}
10^{-10}
10^{-9}
10^{-8}
10^{-7}
10^{-6}
10^{-5}
0
500
1000
1500
2000
Temperature (K)
A
B
C
D
E
Atreya et al. (1981)
Festou et al. (1981)
Hubbard et al. (1995)
Liu and Dalgarno (1996)
Marten et al. (1994)

Figure 2

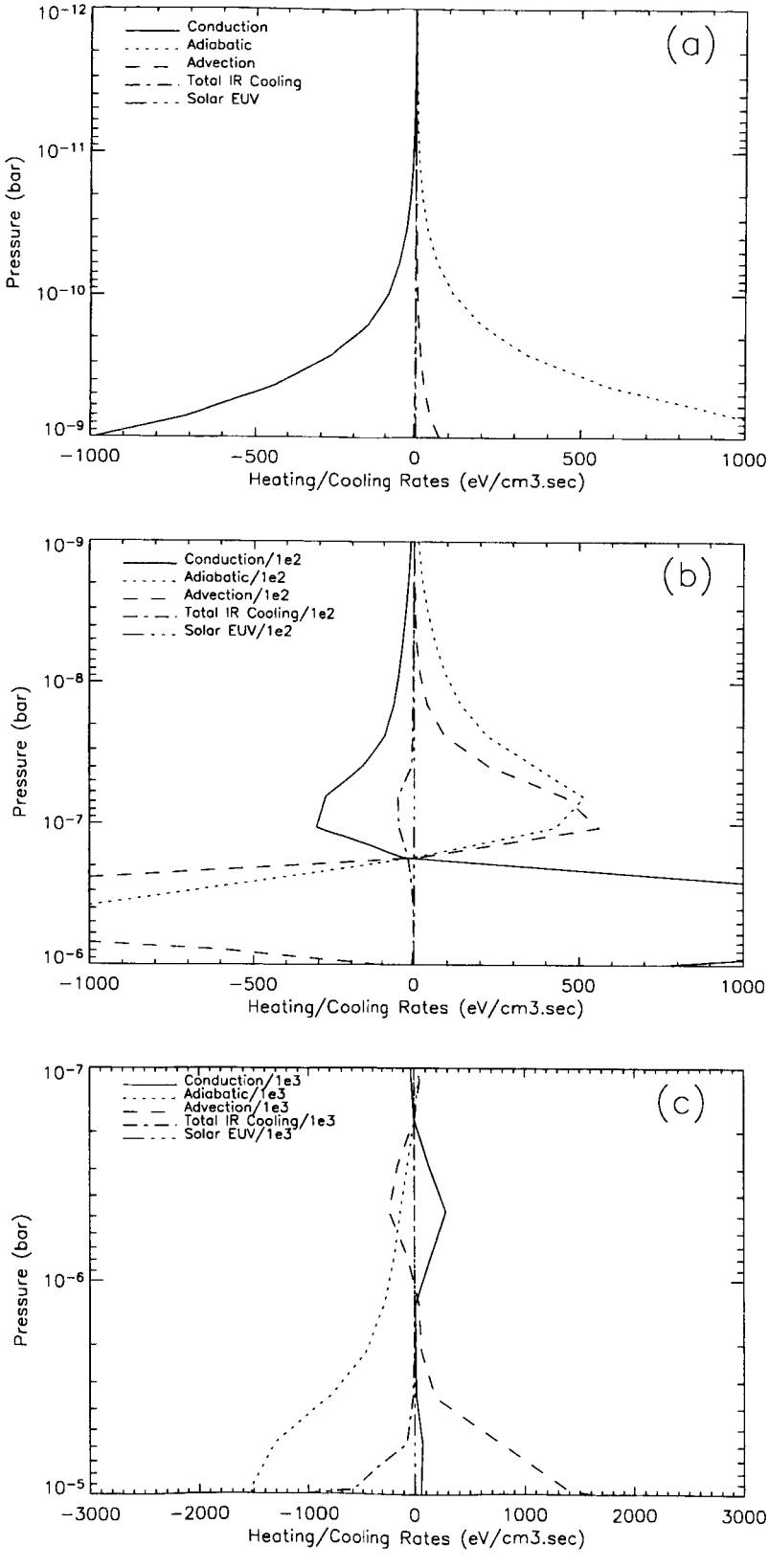
(a)
Conduction
Adiabatic
Advection
Total IR Cooling
Solar EUV
Pressure (bar)
Heating/Cooling Rates (eV/cm3.sec)
(b)
Conduction/1e2
Adiabatic/1e2
Advection/1e2
Total IR Cooling/1e2
Solar EUV/1e2
Pressure (bar)
Heating/Cooling Rates (eV/cm3.sec)
(c)
Conduction/1e3
Adiabatic/1e3
Advection/1e3
Total IR Cooling/1e3
Solar EUV/1e3
Pressure (bar)
Heating/Cooling Rates (eV/cm3.sec)

Figure 3